scientific reports

Check for updates

OPEN

Integrated profiling of adiponectin and cytokine signaling pathways in high-fat diet-induced MASLD reveals early markers of disease progression

Rabia Johnson[1,2,3,7]✉, Samukelisiwe Shabalala[1,4,7], Lawrence Mabasa[1,2], Liske Kotzé-Hörstmann[2,5], Nonhlakanipho Sangweni[1], Pritika Ramharack[1], Jyoti Sharma[1,2], Carmen Pheiffer[1,6], Afolake Arowolo[1] & Hanél Sadie-Van Gijsen[2]

Metabolic dysfunction-associated steatotic liver disease (MASLD), which affects a significant portion of the global population, is linked to high-fat diets (HFD) and characterized by abnormal lipid accumulation and activation of inflammatory pathways in hepatocytes. The precise mechanisms underlying MASLD, especially the involvement of inflammatory cytokines in its pathophysiology, remain unclear. This study evaluated the changes and interactions of steatotic liver and inflammatory markers in an animal model of MASLD by feeding male Wistar rats a high-fat diet (HFD) for 17 weeks. After this period, the serum lipid profiles were assessed, along with liver enzymes, including aspartate aminotransferase (AST) and alanine aminotransferase (ALT). The changes in liver morphology and triglyceride levels were determined by histology and a colorimetric assay, respectively. Steatotic liver and inflammatory markers were measured using a RT^2 Profiler^{TM}PCRArray and validated with quantitative real-time PCR (qRT-PCR). Histological evaluations indicated that HFD livers exhibited macrovesicular steatosis and lobular inflammation. The HFD-fed group had significantly higher hepatic triglyceride levels than the controls (383 ± 23 mg/dL vs. 100 ± 9 mg/dL) and elevated serum lipid levels ($p < 0.0001$), along with increased liver aminotransferase levels. Gene expression analysis showed decreased adiponectin signaling (*AdipoR2*, $p < 0.001$) and upregulated de novo lipogenesis (*Srebf1*, $p < 0.05$). Notably, pro-inflammatory cytokines (*Cxcl10*, *Ccl2*, *Il*β, $p < 0.001$; *TNF-*α, $p < 0.01$) were significantly elevated, correlating with reduced hepatic glucose transporter *Glut2* expression ($p < 0.05$), as confirmed by STRING analysis. These findings demonstrate that HFD consumption alters key genes and pathways involved in adiponectin and insulin signalling, lipogenesis, and inflammatory responses, thereby contributing to the pathogenesis of MASLD. Additionally, it identifies a comprehensive chemokine expression profile, highlighting potential therapeutic targets for MASLD.

Keywords High-fat diet (HFD), Obesity, Non-alcoholic fatty liver disease (NAFLD), Inflammation, Metabolic dysfunction, Steatotic fatty liver diseases (MASLD), Adiponectin

Metabolic dysfunction-associated steatotic liver disease (MASLD), formerly termed non-alcoholic fatty liver disease (NAFLD), affects approximately 30% of the global population, with a higher prevalence in males than

[1]Biomedical Research and Innovation Platform (BRIP), South African Medical Research Council (SAMRC), Tygerberg 7505, South Africa. [2]Centre for Cardio-metabolic Research in Africa (CARMA), Division of Medical Physiology, Faculty of Medicine and Health Sciences, Stellenbosch University, Tygerberg 7505, South Africa. [3]Division of Medical Microbiology, Department of Laboratory-Medicine and Pathology, Faculty of Health Sciences, Walter Sisulu University and National Health Laboratory Services, Mthatha, South Africa. [4]Department of Biochemistry and Microbiology, University of Zululand, KwaDlangezwa 3886, South Africa. [5]Division of Sport and Exercise Medicine, Department of Exercise, Sport and Lifestyle Medicine, Faculty of Medicine and Health Sciences, Stellenbosch University, Tygerberg 7505, South Africa. [6]Department of Obstetrics and Gynaecology, School of Medicine, Faculty of Health Sciences, University of Pretoria, Pretoria, South Africa. [7]Rabia Johnson and Samukelisiwe Shabalala contributed equally to this work. ✉email: rabia.johnson@mrc.ac.za

females[1]. MASLD, defined as an excessive accumulation of fat in the liver, has emerged as the most common chronic liver condition worldwide[2] and is considered the hepatic manifestation of metabolic syndrome. The histological continuum of MASLD spans from uncomplicated steatosis to metabolic dysfunction-associated steatohepatitis (MASH), which can progress to cirrhosis and hepatocellular carcinoma. It has been reported that 30% of patients with MASLD will develop MASH[2]. More importantly, individuals living with MASLD have an increased risk of developing cardiovascular disease (CVD)[3]. The rising prevalence of MASLD is attributed to changes in the lifestyle of Western societies, particularly with the increased consumption of high-fat diets (HFD)[4]. Furthermore, understanding the disease pathophysiology of MASLD is crucial as its global burden closely mirrors the rising rates of obesity, with a MASLD prevalence of 75–80% in obese individuals, compared to just 20–25% in the general population[5]. These striking disease comorbidities, combined with the fact that there are currently no reliable non-invasive biomarkers for the early detection of MASLD[6], underscore the need for a deeper understanding of the underlying mechanisms of MASLD. Experimental evidence has shown that overnutrition and insulin resistance (IR) increase lipolysis, leading to the breakdown of triglyceride (TG) stores and resulting in an enhanced release of glycerol and free fatty acids (FFAs) into the circulation[7]. Additionally, through *de novo* lipogenesis (*DNL*), the liver converts excess carbohydrates into FFAs. The increased FFAs generated are subsequently synthesized into hepatic triglycerides (TGs) at a higher rate, accumulating in hepatocytes and resulting in the development of MASLD. The accumulation of these TGs is facilitated by several genes, including activation of the master regulator of lipid synthesis, Sterol Regulatory Element-Binding-Protein-1c (*Srebp-1c*), which promotes the expression of lipogenic genes such as fatty acid synthase (*Fasn*), Stearoyl-CoA Desaturate1 (*Scd1*), Peroxisome Proliferate-Activated Receptor Gamma (*Ppary*) and acetyl-CoA carboxylase (*Acc*), which catalyse the carboxylation of acetyl-CoA to produce malonyl-CoA, an essential precursor in the synthesis of fatty acids[8,9]. Furthermore, the expression of adiponectin receptors (AdipoR) in the liver also plays a crucial role in mediating the effects of adiponectin, which enhances fatty acid oxidation and improves insulin sensitivity, thereby counteracting lipid accumulation and insulin resistance (IR). While adiponectin is primarily produced in adipose tissue, its favourable effects on liver function are mediated by activating *AdipoR1* and *AdipoR2* receptors. These receptors interact with the adapter protein APPL1, which attenuates inflammatory responses, suppresses fatty acid synthesis, and enhances fatty acid oxidation[10]. Apart from *de novo* lipogenesis (*DNL*), a known consequence of hepatic insulin resistance (IR) and subsequent hepatic TG accumulation and steatosis, inflammation has been implicated as a key mediator of hepatic injury with augmented fibrosis[11]. Consequently, according to the "two-hit hypothesis" proposed by Day (1998), while the first hit causes increased fat accumulation, the second hit triggers intralobular inflammation and fibrosis, further exacerbating tissue injury in MASLD[12,13]. Several studies have also shown that the activation of chemokine and cytokine responses orchestrates hepatic inflammation. For example, the consumption of HFD upregulates proinflammatory cytokines, such as *Tnf-α*and *IL-1β*, via the nuclear factor-kappa-B (NF-κB) pathway, further accelerating disease progression from MASLD to MASH[11,14,15]. Therefore, hepatic inflammation has been identified as a key driver in the development of liver fibrosis[16]. However, the molecular mechanism underpinning MASLD, specifically, the role of inflammatory cytokines, remains to be delineated. Studying MASLD in this context is crucial for identifying novel biomarkers that can inform therapeutic interventions. Therefore, this study aims to elucidate the changes in molecular mechanisms underlying these metabolic changes, with a focus on the dysregulated inflammatory genes and pathways in HFD-induced MASLD.

Materials and methods

Experimental animals

All experimental methods were performed in accordance with the Guide for the Care and Use of Laboratory Animals of the National Institute of Health (NIH, 8th Edition, 2011), the Animal Research: Reporting of *in vivo* Experiments (ARRIVE) guidelines, which were approved by the Animal Research Ethics Committees at Stellenbosch University (SU-ACU-2018-6786) and the University of Zululand (PGD2017/206).

Six-week-old male Wistar rats ($n = 24$) were purchased from the University of Stellenbosch Animal Facility, weighing between 170 and 200 g. They were housed in groups of 4 per cage at the Tygerberg Animal Research Facility (Faculty of Medicine and Health Sciences, Stellenbosch University). Animals were kept in a controlled environment with a 12-hour artificial dark/light cycle and maintained at a temperature range of 23–25°C with a relative humidity of 50%. Throughout the acclimation period, all animals were provided with standard rat chow and had unrestricted access to drinking water and food.

Dietary administration

Animals were randomized into two groups ($n = 12$/group) and fed either a standard rat chow diet (Control) or HFD (high fat/fructose/cholesterol with 66% energy from fat) (Supplementary Table S1). After 17 weeks on the prescribed diet, the animals were euthanized to assess the effect of diet on liver function. Our previous work has extensively discussed and described the composition and metabolic consequences of the control (standard rat chow diet) and HFD[17,18].

Sample collection

After 16 weeks in their respective dietary groups, the rats were fasted overnight, and 1 mL of blood was subsequently collected from the jugular vein into BD Vacutainer® serum separator tubes (SST) (Becton Dickinson, Berkshire, UK)[17]. Coagulation was achieved by incubation for 1 h on ice. Serum was collected by centrifugation at 4000 g for 10 min at 4 °C, and the resulting serum fraction was transferred to a microcentrifuge tube and stored at -80 °C until analysis of the serum lipid profile. At the endpoint of the study (17 weeks), animals were euthanized in a non-fasted state. The euthanasia process involved administering sodium pentobarbitone (Bayer, South Africa) via intraperitoneal injection at a dose of 160 mg/kg. This dose was selected to induce

deep anesthesia followed by humane euthanasia, ensuring a rapid and painless process, and is in line with the 2020 American Veterinary Medical Association (AVMA) guidelines for the euthanasia of animals. The liver tissues were excised and either placed in RNALater (ThermoFisher Scientific, Inc., Waltham, MA, USA) for subsequent mRNA expression analysis or formalin-fixed and paraffin-embedded for Hematoxylin and Eosin (H&E) staining.

Quantification of hepatic triglycerides

Total liver TG was extracted using a modified Folch extraction method[19]. Briefly, 225 mg of tissue was added to 450 µL saline and homogenized for 5 × 1 min at 25 Hz (Qiagen TissueLyser II Bead Mill, USA). After this step, 0.8 volume of sample was added to 2 volumes of methanol (M) and 1 volume of chloroform (C). The sample was then vortexed for 20 min at room temperature (RT) to disrupt the lipid droplets. Then, a saturated chloroform: methanol: saline (CMS) mixture in a ratio of 86:14:1 was made before centrifugation at 5000 rpm for 10 min at 4 °C to separate the phases. The bottom yellow lipid phase was then transferred to a clean tube, and 2 x CMS with butanol was added, followed by 15 s of vortexing and centrifugation at 5000 rpm for 10 min at 4 °C. The diluted lipids were then transferred to a new tube and dried under nitrogen gas for long-term storage at -80 °C or dissolved in ethanol containing 1% Triton-X 100 for subsequent enzymatic colorimetric measurements of total TGs using the LabAssay™ Triglyceride kit (catalog number 632-50991, Wako Chemical, Germany), as per manufacturer's instructions.

Histopathological analysis

Liver sections were kept in a 10% formalin solution and embedded in paraffin blocks. Tissue blocks were sliced into 10-µm sections using a cryostat and fixed onto glass slides coated with aminopropyltriethoxysilane, obtained from Sigma-Aldrich Corp., St. Louis (catalogue number 440140). Subsequently, these sections were stained with Hematoxylin and eosin (H&E). The stained sections were then sent to IDEXX Laboratories (Kyalami Village, Johannesburg, South Africa), where liver pathology assessment was performed.

Quantitative real-time polymerase chain reaction analysis (qRT-PCR) using PCR arrays

Total RNA was extracted from liver tissues using TRIzol reagent, as per the manufacturer's instructions (ThermoFisher Scientific, Inc., Waltham, MA, USA). Thereafter, the Turbo DNase Kit (ThermoFisher Scientific) was used to remove genomic DNA, as per the manufacturer's instructions. Two micrograms of RNA were used for first-strand complementary DNA (cDNA) synthesis, which was performed using a QuantiTect Reverse Transcription First-Strand cDNA Synthesis Kit (Qiagen, Hilden, Düsseldorf, Germany), according to the manufacturer's instructions. Thereafter, differential gene expression analysis was carried out using the pre-designed RT^2 Profiler™ PCR Arrays for Rat Fatty Liver (catalog number 330231; GeneGlobe ID PARN-157Z) and Rat Cytokines and Chemokines Profiler Arrays (catalog number 330231; GeneGlobe ID PARN-150Z) on the QuantStudio™ 7-Flex Real-Time PCR instrument (ABI) instruments, Life Technologies, USA). Analysis of PCR array data was performed online using the GeneGlobe Design and Analysis web portal (https://dataanalysis.qiagen.com/pcr/arrayanalysis.php). Gene expression was quantified using the ΔΔCt method. Arrays had a cut-off Ct value of 35 cycles, and the expression data were normalized against Lactate dehydrogenase A (*Ldha*) and ribosomal protein lateral stalk 1 (*Rplp1*).

TaqMan® gene expression analysis

One microgram of RNA was reverse-transcribed using the Life Technologies High-Capacity Reverse Transcription kit, according to the manufacturer's instructions (ThermoFisher Scientific, catalog number 4368841). Real-time polymerase chain reaction was performed using 1 µL of cDNA, 5 µL of TaqMan Fast Advanced Master Mix, and 0.5 µL of TaqMan gene expression assay in a 10 µL reaction volume. TaqMan® gene expression assays used in qRT-PCR analysis included Adiponectin receptor 1 and 2 (*AdipoR1 and 2*,) (Rn01483784_m1 and Rn01463173_m1), Adaptor protein, phosphotyrosine interacting with PH domain and leucine zipper 1 (*Appl*) (Rn01401841_m1), AMP-activated protein kinase (*Ampk*) (Rn00576935_m1), peroxisome proliferator-activated receptor alpha (*Pparα*) (RN07311525_m1), chemokine (C-C motif) ligand 2 (*Ccl2*) (Rn00580555_m1), C–X–C motif chemokine 10 (*Cxcl10*) (Rn00594648_m1), interleukin-1-beta (*IL1β*) (Rn00580432_m1), interleukin-12B (*IL12b*) (Rn00575112_m1), sterol regulatory element binding transcription factor 1 (*Srebf1*) (Rn00562055_m1) and Tumor necrosis factor-alpha (*TNF-α*). Beta-actin (*Act-β*) (Rn00667869_m1) and Hypoxanthine-guanine phosphoribosyltransferase 1 (*Hprt1*) (Rn01527840_m1) were used as endogenous controls. The Applied Biosystems QuantStudio™ 7-Flex Real-Time PCR System (ABI instruments, Life Technologies, USA) was used to run the qRT-PCR experiments with the thermal experimental conditions as follows: Uracil-N-Glycosylase (UNG) activation was performed at 50 °C for 10 min, enzyme activation at 95 °C for 3 min, a 40-cycle amplification at 95 °C for 15 s and annealing/extending at 60 °C for 1 min. The gene expression levels were calculated using the standard curve method and normalized to endogenous controls.

Gene interaction analysis

The Search Tool for the Retrieval of Interacting Genes/Proteins (STRING) analysis (http://string-db.org/) was used to evaluate the known and predicted protein-protein interactions of the differentially expressed genes (DEGs). The minimum interactive score was set at a high confidence (0.7).

Statistical analysis

Results were expressed as the mean ± standard error of the mean (SEM) of ten to twelve animals per group. Fold change was used to represent data for relative mRNA expression. Statistical analysis was performed using GraphPad Prism® version 9 (GraphPad Software Inc., La Jolla, CA, USA). Differences between the two groups

were analyzed using Student's t-test. Both Student's t-test and Wilcoxon rank-sum test for nonparametric analysis were employed when applicable. A p-value of < 0.05 was considered statistically significant.

Results

HFD causes hepatic steatosis

Histological analysis of H&E-stained sections of control diet-fed rats exhibited a typical liver morphology typified by hepatocytes with round nuclei and centrally located nucleoli (Fig. 1A, white arrows) with flat endothelial cells (black solid arrow). In contrast, the livers of HFD-fed animals exhibited macrovesicular steatosis (Fig. 1B), characterized by enlarged, clear lipid vacuoles (green arrows) with the nucleus displaced toward the periphery of the cell (white arrow), and liver cells having indented nuclei (orange arrows). Mild lobular inflammation was visible, with a few clusters of mononuclear leukocytes (black dashed arrows) and ballooning (red arrow) (Fig. 1B). Hepatic TG levels validated the observation made using H&E staining, with increased liver TG content observed in the HFD-diet group as compared to the control diet group (383 ± 23 mg/dL vs. 100 ± 9 mg/dL,

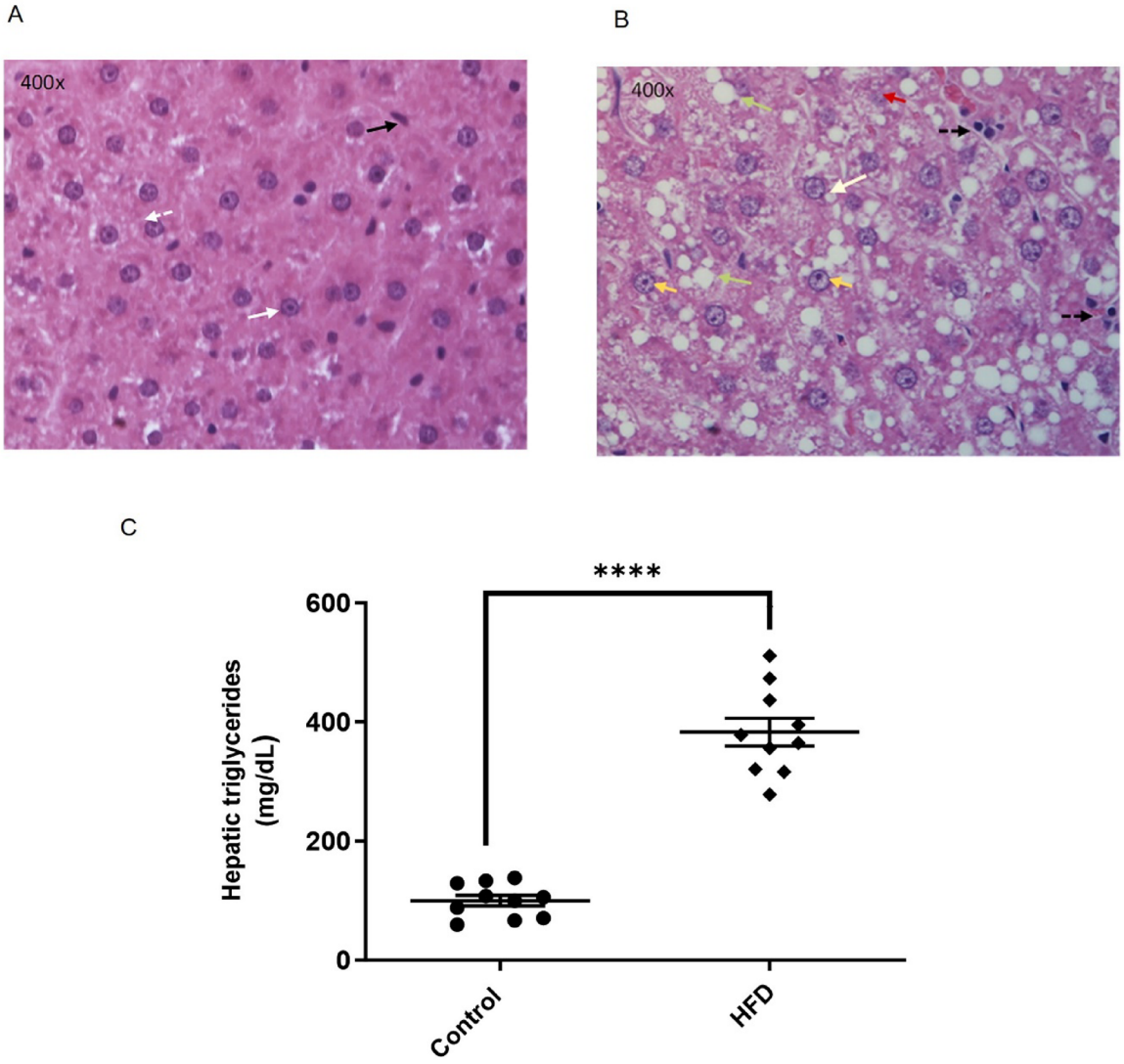

Fig. 1. Hematoxylin and Eosin (H&E) stained sections and hepatic triglycerides measurements of Wistar rats fed a high-fat diet. (**A**) A typical liver tissue section from Wistar rats fed a control diet. Nuclei are round and centrally placed with a prominent nucleolus (white solid arrow) with flat endothelial cells (black solid arrow), which is common in healthy liver tissue. (**B**) In HFD-fed animals, large empty vacuoles are observed (green arrow). Fatty changes are mostly macrovesicular steatosis with the nucleus pushed to the side (white arrow) and hepatocytes filled with indented nuclei (orange arrows). Mild lobular inflammation can be seen, as indicated by the broken black arrow, and a solid red arrow indicates balloon cells. Liver sections were stained with hematoxylin and eosin, and all photomicrographs were taken at 400x magnification. (**C**) Bar graph quantifying hepatic triglyceride levels per tissue weight (mg). Results are represented as mean ± standard error of the mean (SEM) of $n = 10–12$ animals per group. Comparisons between groups were performed using Student's t-test t. **** = $p \leq 0.0001$.

$p < 0.0001$), which also corresponded to an increase in liver mass in the HFD group compared to the control diet group (Fig. 1C).

HFD increased serum lipid and liver enzyme profiles

As previously reported[17], rats on the HFD exhibited a 60% increase in serum cholesterol levels and a 117% increase in serum triglyceride levels compared to the control dietary group (Table 1). Moreover, serum LDL levels were 65-fold higher in the HFD group compared to the control (Table 1, data originally published in[17]).

Similarly, AST and ALT, which are known serum markers of liver injury. The reference ranges of AST and ALT are 50–96 IU/L and 24–49 IU/L, respectively, in the serum of healthy male Wistar rats[20]. Serum AST was significantly elevated in the HFD group compared to the control diet group (171 ± 20 compared to 103 ± 5.4, IU/L $p < 0.0001$). Likewise, HFD-fed rats displayed significantly increased ALT levels compared to the control (134 ± 16 versus 36 ± 1.3 IU/L $p < 0.0001$) (Supplementary Fig. 1), indicating the onset of hepatic steatosis[21].

In vivo effect of an HFD diet on gene expression

Gene expression analysis was performed on RNA extracted from liver tissue to elucidate the molecular mechanisms induced by the consumption of the HFD used in this study. Of the 168 genes assessed, 51 (29%) were differentially expressed, with 31 linked to an inflammatory response, 2 to apoptosis, 10 to *DNL*/adiponectin signalling, and 8 to insulin signalling (Table 2). STRING analysis depicted an interaction between genes involved in DNL, IR, and inflammation. Notably, the interaction of Peroxisome Proliferator-Activated Receptor Gamma (Pparγ) with proteins linked to *de novo* lipogenesis, including *Sterol Regulatory Element-Binding Transcription Factor 1 (Srebf1)*, *Lipoprotein Lipase (Lpl)*, and Stearoyl-CoA Desaturase *(Scd)*, with an interaction score of 0.7, indicating a strong interaction (Fig. 2).

HFD dysregulates the expression of lipid metabolism-related genes

During the consumption of HFD, *DNL* is the earliest response that contributes towards fat accumulation in the liver[22]. Our findings showed that there was a significant increase in the expression of lipid metabolism genes (*Fabp5*, *Pparγ*, *Scd1*, *Strebf1*, *PA1*, $p < 0.05$), inflammation/fibrosis gene (*Lpl*, 4-fold, $p < 0.05$), and an increase in the cholesterol transport gene, *Abcg1* (> 5-fold, $p < 0.001$) (Table 2). Conversely, a significant decrease in adiponectin receptor expression, specifically *AdipoR2 ($p < 0.001$)*, was observed. STRING analysis confirmed a strong interaction of *Pparγ* with proteins linked to *DNL*, including *Srebf1*, *Lpl and Scd1* (Fig. 2).

HFD dysregulates the expression of glucose metabolism and insulin signalling-related genes

As fat accumulates in hepatocytes, insulin signalling pathways are interrupted, impairing glucose metabolism in the liver[47]. In this study, we observed a modest but significant increase in the expression of *Fas* and the lipid accumulation gene, *G6pd* (1.76-fold, $p = 0.02$), as well as the insulin signalling response gene *Ptpn1* (2-fold, $p < 0.001$), in response to the HFD, whilst the expression of Glut2 encoding gene, *Slc2a2*, was decreased (-1.55-fold, $p < 0.01$) (Table 2). The overall downregulation of *Irs1*, *Insr*, *Pi3k*, and *Glut2* in the liver is often associated with impaired glucose metabolism and systemic insulin resistance, which are key features of Type II diabetes mellitus[48]. STRING analysis indicated that these genes/proteins have strong interactions, suggesting biological and functional connections, with *G6pd* being linked to *Srebf1*. The coloured lines between the nodes indicate functional and physical protein interaction with a minimum interaction score of 0.70 (high confidence) (Fig. 3).

HFD increases the activation and expression of inflammatory chemokines/cytokines and genes

As hepatic steatosis and insulin resistance progress, an inflammatory response is triggered[49]. Results showed that the consumption of the HFD resulted in the increased gene expression of factors involved in the recruitment of immune cells, including monocytes, macrophages, T cells, and neutrophils (*Ccl12*, *Ccl17*, *Ccl19*, *Ccl21*, *Ccl22*, *Ccl3*, *Ccl2*, *Ccl4*, *Ccl7*, *Cx3cl1*, *Cxcl1*, *Cxcl10*, *Cxcl13*, *Cxcl16*, *Cxcl3* and *Cxcl9* (> 2-fold, $p < 0.001$) (Table 2). This response can contribute to hepatocyte injury and fibrosis, which are critical features of MASLD[14]. Furthermore, it was observed a significant increase in cytokine response with Ifnγ, *Tnfα*, *Il1b*, *Il6*, *Il10*, *Il12b*, *Il17a*, *Il18*, *Il1rn*, *Il21*, *Il27*, *Il16* and *Il17* being upregulated (> 2-fold, $p < 0.001$), which would further exacerbate IR, inflammation and fibrosis in the liver[41]. Moreover, STRING analysis confirmed an interaction between the DNL, Insulin signalling pathways and activation of the chemokine and cytokine pathways (Fig. 4).

Variable (Unit)	Control	HFD	*p*-value
Total cholesterol (mmol/L)	1.9 ± 0.087	3.1 ± 0.190	0.0001
Triglycerides (mmol/L)	0.60 ± 0.034	1.3 ± 0.110	0.0001
LDL (mmol/L)	0.02 ± 0.009	1.3 ± 0.140	0.0001
AST (IU/L)	103 ± 5.400	171 ± 20.000	0.0001
ALT (IU/L)	36 ± 1.300	134 ± 16.000	0.0001

Table 1. The effect of HFD diet on serum lipids levels and liver enzyme activity. Results are expressed as the mean ± SEM, n=10–12 rats per group. Differences between groups were assessed using parametric t–tests for data with a normal distribution. Data was originally published in[17] and reproduced here for clarity.

Gene name	Gene symbol	Fold regulation	*p*-value	Function
Chemokines involved in the recruitment of macrophages				
C-C motif chemokine 12	*Ccl12*	4.23	0.001053	The recruitment of monocytes that will differentiate into macrophages. Macrophage infiltration will result in the activation of a proinflammatory response. Increased CCL levels in MAFLD lead to the recruitment of monocytes, which contribute to liver inflammation and damage[23,24].
C-C motif chemokine 17	*Ccl17*	5.20	0.002796	
C-C motif chemokine 19	*Ccl19*	2.16	0.000075	
C-C motif chemokine 21	*Ccl21*	5.36	0.000122	
C-C motif chemokine 22	*Ccl22*	5.11	0.0000001	
C-C motif chemokine 3	*Ccl3*	7.03	0.000024	
C-C motif chemokine 4	*Ccl4*	4.16	0.000173	
C-C motif chemokine 7	*Ccl7*	11.09	0.000022	
C-C motif chemokine 2	*Ccl2*	10.24	0.000002	
Granulocyte-macrophage colony-stimulating factor	*Csf2*	8.03	0.000006	Reduces intrahepatic fat accumulation and inflammation in animal models of NAFLD[25].
Fractalkine	*Cx3cl1*	3.58	0.000059	The increase of chemokines and attraction of immune cells, particularly T cells and neutrophils, to the liver increases fibrosis during MAFLD[23,24,26].
C-X-C motif chemokine ligand 10	*Cxcl1*	6.44	0.0000001	
C-X-C motif chemokine ligand 10	*Cxcl10*	10.46	0.000019	
C-X-C motif chemokine ligand 13	*Cxcl13*	3.76	0.000018	
C-X-C motif chemokine ligand 16	*Cxcl16*	8.82	0.00005	
C-X-C motif chemokine ligand 3	*Cxcl3*	12.89	0.000279	
C-X-C motif chemokine ligand 9	*Cxcl9*	14.11	0.000039	
Cytokines				
Interferon-gamma	*Ifnγ*	25.84	0.000194	Increase inflammation and proinflammatory cytokines during MAFLD development[27].
Tumor necrosis factor-alpha	*Tnfα*	9.76	0.000113	Inflammatory mediators involved in the development of MAFLD[28].
Interleukin-1beta	*Il1b*	6.09	0.000001	
Interleukin-6	*Il6*	4.20	0.002197	
Interleukin-10	*Il10*	8.44	0.000833	Suppresses the production of proinflammatory cytokines (like *Tnf-α*, *Il-1β*, and *Ifnγ*). Prevents excessive immune activation and inflammation, which can lead to liver damage[29,30].
Interleukin-12beta	*Il12b*	8.40	0.000001	Influences insulin sensitivity and contributes to insulin resistance, a critical factor in the development of MAFLD[31].
Interleukin-17alpha	*Il17a*	2.87	0.00318	Stimulates macrophage activation and increases fibrosis[32].
Interleukin-18	*Il18*	2.54	0.000106	Pro-inflammatory role in NAFLD[33].
Interleukin-1receptor antagonist	*Il1rn*	2.25	0.000562	Interacts with metabolic pathways and the potential influence of insulin sensitivity[34].
Interleukin-21	*Il21*	7.36	0.000569	
Interleukin-27	*Il27*	4.25	0.00084	Promotes anti-inflammatory effects, reduces liver damage, by activating Treg cell responses[35].
Interleukin-16	*Il16*	2.36	0.000004	Not typical driver of IR but involved in the inflammation process of IR[34].
Interleukin-4	*Il4*	−2.30	0.022736	
Interleukin-7	*Il7*	3.69	0.000001	
Apoptosis				
Fas ligand	*Faslg*	2.27	0.01726	Regulates apoptosis[36].
Caspase-3	*Casp3*	1.58	0.000132	Increases tissue damage and liver scarring or contributes to hepatocellular carcinoma[37]
Regulation of lipogenesis				
Fatty acid-binding [rotein 5	*Fabp5*	2.94	0.002083	Involved in *de novo* fatty acid synthesis. SCD1 increases the production of monounsaturated fats, which contribute to lipid dysregulation and insulin resistance[38].
Fatty acid synthase	*Fas*	1.73	0.001234	
PPARγ (Peroxisome proliferator-activated receptor gamma	*Pparg*	1.59	0.007636	
Stearoyl-CoA desaturase 1	*Scd1*	1.50	0.0587304	
Sterol regulatory element-binding protein (SREBP)-1c	*Srebf1*	1.46	0.024681	
Lipoprotein lipase	*Lpl*	4.02	0.000001	Increased LPL expression results in augmented fatty acid delivered to the liver, increasing the development of MAFLD[39].
Plasminogen activator inhibitor-1	*Serpine1/PAI-1*	5.39	0.002471	Diagnostic indicator of NASH progression[40].
Nuclear factor-kappaB	*Nfkb1*	1.38	0.026722	Transcription factor with a role in chronic inflammation that contributes to IR[41].
ATP-binding cassette sub-family G member 1	*Abcg1*	5.27	0.000001	Facilitates efflux of cholesterol from hepatocytes (dysfunction contributes to liver steatosis)[42].
Continued				

Gene name	Gene symbol	Fold regulation	*p*-value	Function
Adiponectin receptor 2	*Adipor2*	−1.58	0.000001	Improves liver insulin sensitivity, thereby regulating glucose and lipid metabolism[10].
Insulin signalling				
Insulin receptor	*Insr*	−1.28	0.000019	Role in insulin signalling. Decreased levels play a role in the impairment of insulin signalling. As a result, glucose uptake and glycogen synthesis are reduced[43].
Insulin receptor substrate 1	*Irs1*	−1.39	0.000001	
Phosphatidylinositol-4,5-bisphosphate 3-kinase catalytic subunit	*Pik3ca*	−1.35	0.000003	
Phosphatidylinositol-4,5-bisphosphate 3-kinase catalytic subunit	*Pik3r1*	−1.20	0.000576	
Solute carrier family 2 member 2 (Glucose transporter 2 encoding gene)	*Slc2a2*	−1.55	0.000002	Glucose-sensing glucose transporter[44].
Protein tyrosine phosphatase 1B	*Ptpn1*	2.10	0.000078	Negatively regulates insulin signalling by dephosphorylating key proteins in the signalling pathway[45].
Glucose-6-phosphate dehydrogenase	*G6pd*	1.76	0.021564	Facilitates glucose metabolism via the pentose phosphate pathway; improves oxidative stress.
Glucose-kinase	*Gck*	−1.05	0.00173687	Converts glucose into glycogen. But, during insulin resistance, the liver's response to insulin becomes impaired[46].

Table 2. Summary of results for differentially expressed genes (DEGs) identified with PCR array analysis (shown as fold-change in HFD-fed animals, compared to control diet-fed animals).

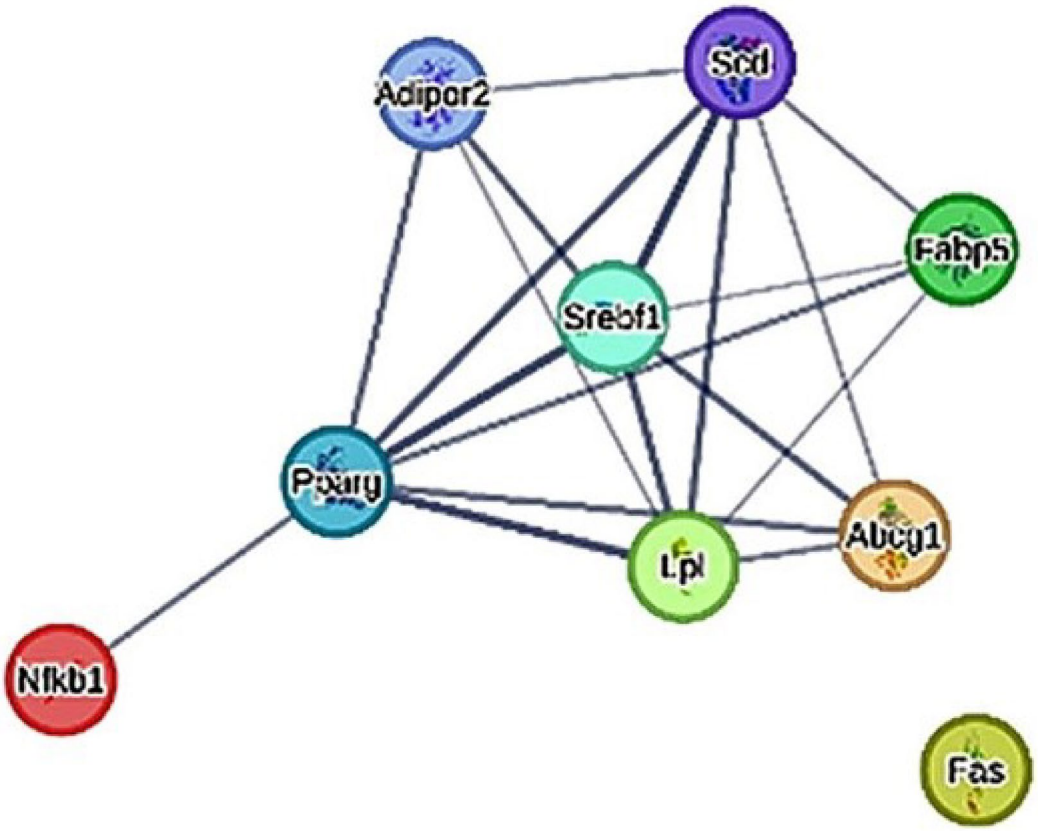

Fig. 2. HFD induces hepatic lipid accumulation by activating key lipid metabolism genes. Search Tool for the Retrieval of Interacting Genes/Proteins analysis (STRING) analysis demonstrated the significant interaction of Peroxisome Proliferator-Activated Receptor Gamma (Pparγ) with proteins linked to *de novo* lipogenesis, including Sterol Regulatory Element-Binding Transcription Factor 1 (Srebf1), Lipoprotein Lipase (Lpl) and Stearoyl-CoA Desaturase (Scd). The thickness of the lines between the nodes indicates the strength of the data support with a minimum interaction score of 0.70 (high confidence).

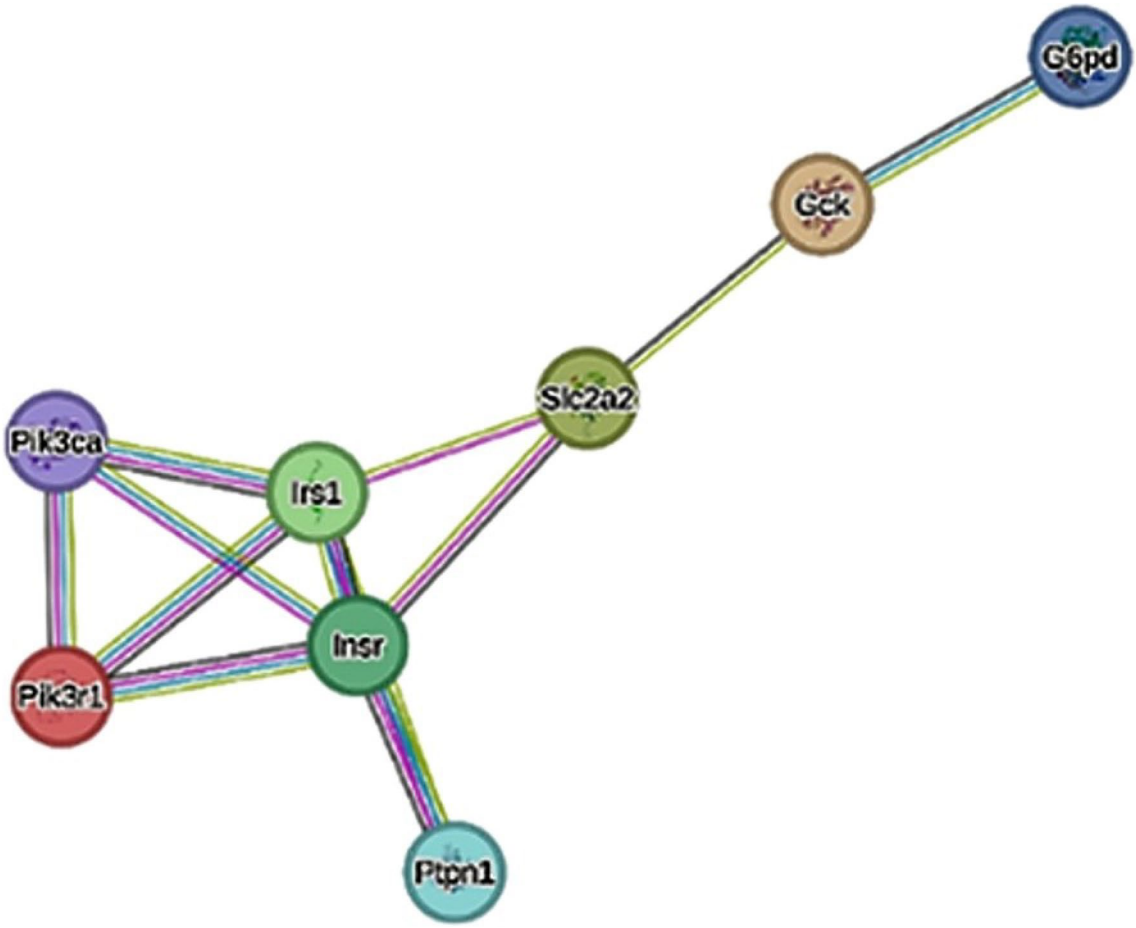

Fig. 3. High fat diet disrupts Insulin signalling Pathway. Search Tool for the Retrieval of Interacting Genes/Proteins analysis (STRING) analysis confirmed a strong interaction between differentially expressed genes and known protein-protein interaction in the insulin signalling pathway.

Validation of specific differentially expressed genes from the PCR array analyses

Following PCR array experiments and data analysis, validation of specific differentially expressed genes in the HFD group compared to the control diet group was conducted using qRT-PCR. The focus was placed on genes linked to adiponectin signalling (Ppar-α, Ampk, AdipoR1, and AdipoR2), DNL (*Srebf1* and *Glut2*), and inflammation (*Il1β*, *Tnf-α*, *Ccl2, and Cxcl10*) pathways that exhibited a substantial degree of differential expression. It was observed that 17 weeks of HFD resulted in a significant downregulation of crucial genes associated with adiponectin signalling, including AdipoR1 ($p < 0.0001$), *AdipoR2* ($p < 0.0001$), *AMPK* ($p < 0.0001$), and *PPARα* ($p < 0.05$) (Fig. 5A–D). In genes involved in DNL, the expression of *Glut2* was markedly downregulated ($p < 0.001$), while that of *Srebf1* was upregulated ($p < 0.05$) (Fig. 6A,B). Lastly, the expression of pro-inflammatory response genes was significantly increased (*Cxcl10* ($p < 0.001$), *Ccl2* ($p < 0.001$), *Tnf-α*($p < 0.01$) and *Il1β* ($p < 0.001$)) (Fig. 7A–D), when compared to the control diet group.

Discussion and conclusion

Over the last two decades, the global prevalence of MASLD has increased by 50%[50], with several studies demonstrating that long-term HFDs elevate the risk of hepatic steatosis[4]. Metabolic dysfunction-associated steatotic liver disease is an asymptomatic condition, and its advancement into MASH and subsequent hepatocellular carcinoma contributes to its increased morbidity and mortality. *De novo* lipogenesis (DNL), insulin resistance (IR), and chronic inflammation contribute to these risks; therefore, MASLD is recognized as the hepatic manifestation of metabolic syndrome. No serum biomarkers for early detection have been identified to date[6], and non-invasive methods of diagnosis, disease progression, and monitoring of response to treatment form the cornerstone of MASLD management[6]. Furthermore, the full contribution of the inflammatory pathway to MASLD remains understudied. As such, understanding the disease pathophysiology of HFD-induced MASLD, particularly in the context of chronic inflammation, is crucial for identifying viable biomarkers for pharmacological intervention. Hence, this study investigated the molecular mechanisms associated with the development of MASLD, focusing on dysregulated inflammatory genes and pathways, to identify such biomarkers.

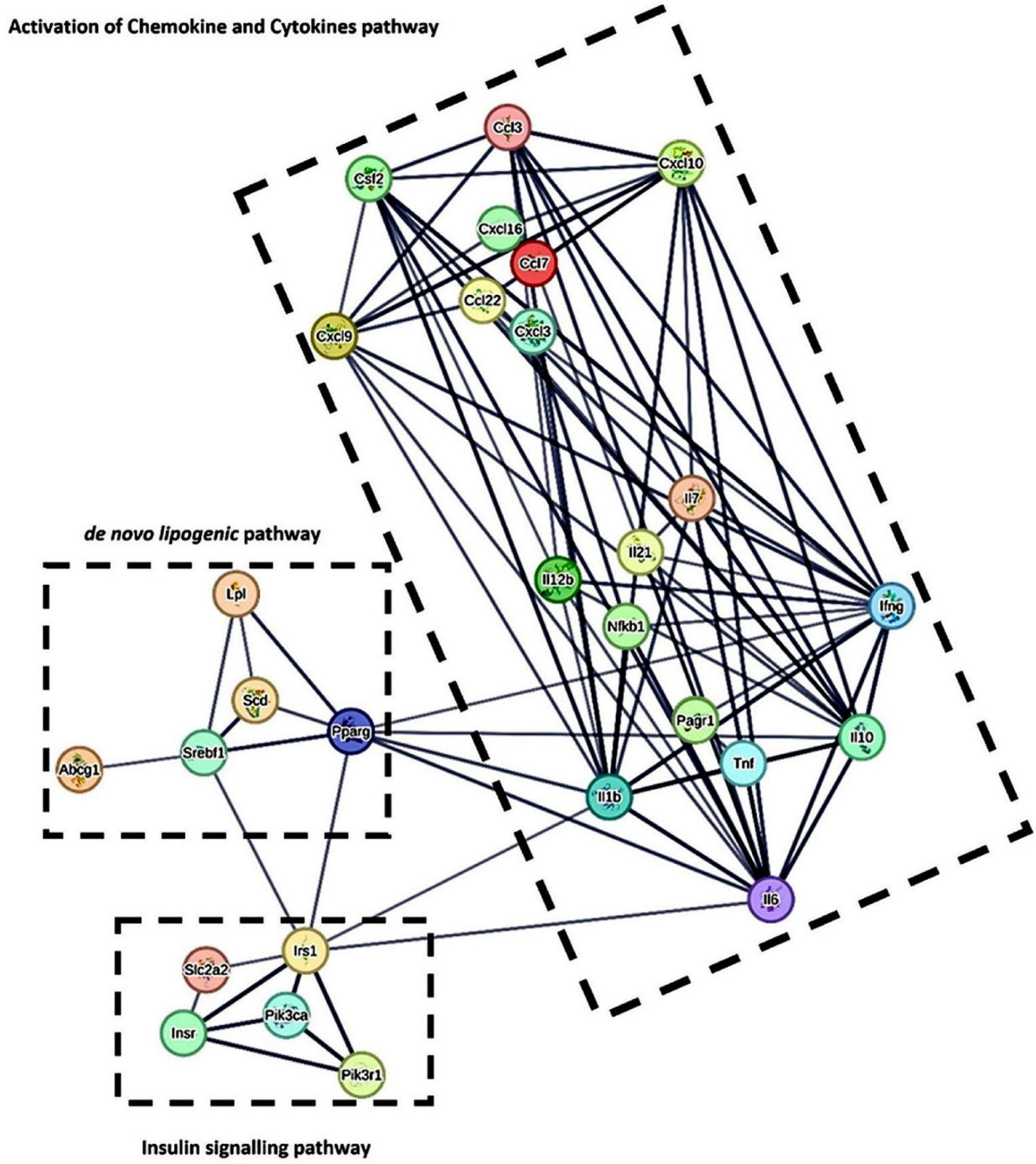

Fig. 4. Molecular mapping of HFD-induced liver inflammation and metabolic dysregulation HFD induced liver steatosis through activating key inflammatory and lipid metabolism genes. Search Tool for the Retrieval of Interacting Genes/Proteins analysis (STRING) analysis confirmed the major interaction of Peroxisome Proliferator-Activated Receptor Gamma (*Pparγ*) with proinflammatory cytokines, including tumour necrosis factor-α (*Tnf-α*), Interferon-gamma γ *(Ifn-γ)*, interleukin2/1β/6 (*ll-2*, *Il-1β*, *Il-6*), leading to the initiation of Nuclear Factor kappa-light-chain-enhancer of activated B cells (*Nf-kb*) regulation. PPARγ also enhanced the expression of proteins linked to lipid absorption, TG storage, and the development of lipid droplets, such as fatty acid binding protein (*Fabp*). Transcription factors that play a role in lipid metabolism and glucose homeostasis, such as sterol regulatory element binding transcription factor 1 (*Srebf1*), stearoyl-CoA desaturase 1 (*Scd1*) and Pparγ were linked to key processes in the insulin signalling pathway (Insulin receptor substrate-1 (*Insr1*), Phosphatidylinositol 3-kinase, catalytic alpha polypeptide (*Pik3ca*), Phosphatidylinositol 3-kinase, regulatory subunit 1 alpha (*Pi3k3r1*), glucose transport (Solute Carrier Family 2, member 2 (Slc2a2)/Glut2) and inflammation. Interferon-gamma (Ifn-γ) is a major proinflammatory cytokine that promotes fibrogenesis in the liver by activating hepatic stellate cells, which are involved in fibrosis formation. It has been well reported that *Ifn-γ* induces a cytokine storm that results in the progression of liver fibrosis[49].

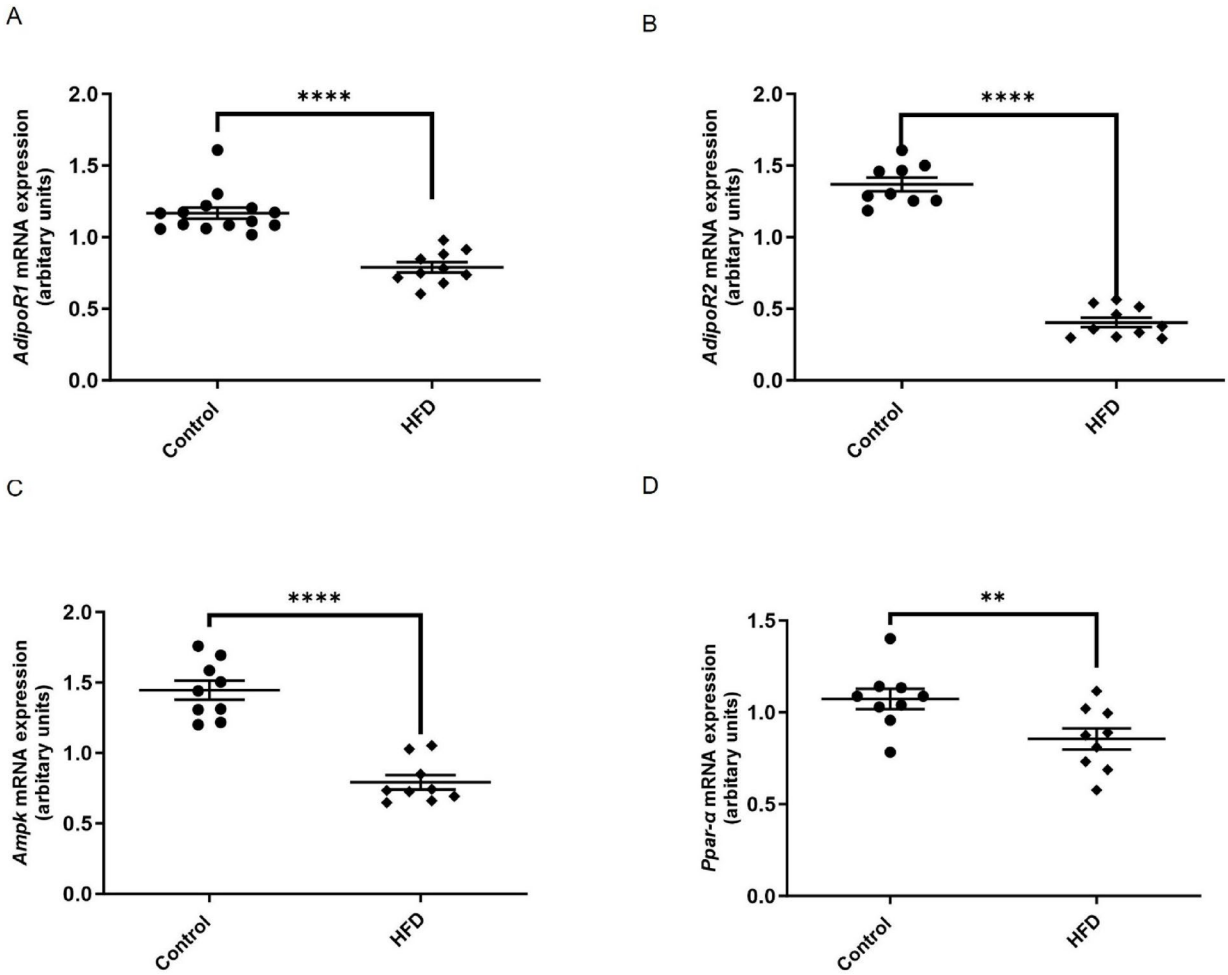

Fig. 5. HFD downregulates vital genes involved in adiponectin signaling. HFD-fed Wistar rats presented with a decreased gene expression of *AdipoR1* (**A**), *AdipoR2* (**B**), AMP-activated protein kinase (*Ampk*) (**C**) and peroxisome proliferator-activated receptor alpha (*Pparα)* (**D**). The findings are displayed as mean ± SEM. Significance levels are as follows: * $p \leq 0.05$, **** $p \leq 0.0001$ compared to the control diet-fed rats.

The pathogenesis of HFD-induced liver injury is complex, involving a network of genes that regulate lipid metabolism, IR, inflammation, fibrosis, and apoptosis. The initial response in MASLD development is characterized by the accumulation of triglycerides in the liver, resulting in the formation of clear vacuolated nuclei, which is subsequently followed by the progression of macrovesicular steatosis, ballooning, and lobular inflammation, ultimately leading to mild to advanced fibrosis and potentially culminating in liver cirrhosis[51]. The present study demonstrated that 17 weeks of HFD exposure in rats led to enhanced triglyceride accumulation in the liver, accompanied by macrovesicular steatosis, characterized by hepatocytes with indented nuclei and mild lobular inflammation, consistent with the histological features of MASLD and MASH described elsewhere[51]. Similarly, Xu et al. reported that after 12 weeks of HFD feeding, rats developed hepatic changes consistent with moderate to severe steatosis and inflammation, while abnormal liver function and fibrosis were apparent after 16 weeks[52]. In this study, it was also found that 17 weeks of feeding with HFD increased AST, ALT, total cholesterol and LDL levels, providing further evidence of liver injury and dysfunction. At a molecular level, the demonstrated upregulation of various pathways associated with DNL, inflammation, and insulin resistance was consistent with findings described elsewhere[11,14,15]. Adiponectin, through activation of its receptors *AdipoR1* and *R2* in the liver, enhances insulin sensitivity and protects against unfavourable metabolic sequelae of *DNL* and MASLD[53]. *De novo* lipogenesis is often an early event in MASLD development when excessive carbohydrate and fat intake result in the accumulation of fatty acids and triglycerides[54]. Activation of AdipoR1 promotes AMPK activation, while AdipoR2 stimulates PPARα activation; however, both pathways contribute to fatty acid oxidation and decreased lipid synthesis in the liver[55]. We observed HFD-mediated downregulation of *AdipoR1*, *AdipoR2*, *Ampk* and *PPARα*, together with upregulation of genes involved in lipid synthesis and lipid accumulation (*Fabp5*, *Pparg*, *Scd1*, *Srebf1* and *Lpl*), indicating a coordinated loss of the protective effects of adiponectin and upregulation of DNL. We also observed the downregulation of various components of the insulin receptor signalling pathway, which may have contributed to hepatic insulin resistance. Although insulin receptor signalling has been shown to upregulate SREBP1[56], we observed mildly increased SREBP1 expression amidst the *downregulation* of insulin

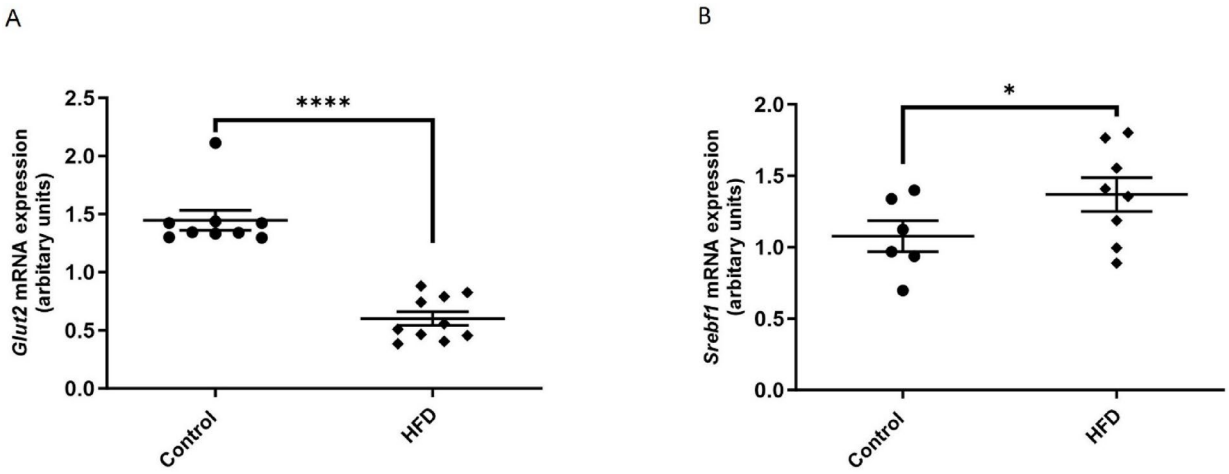

Fig. 6. Differential expression of specific genes involved in glucose transport and DNL during HFD-induced MALFD. Wistar rats fed with HFD presented with a decreased gene expression of the liver-specific glucose transporter 2 (G*lut*2) (**A**) and increased expression of sterol response element-binding protein (*Srebf*1) (**B**). The findings are displayed as mean ± SEM. Significance levels are as follows: * $p \leq 0.01$, **** $p \leq 0.0001$ compared to the control rats.

receptor signalling. Furthermore, HFD-fed rats in the present study exhibited downregulated expression of Glut2, the glucose-sensing transporter in the liver. This reduction in Glut2, together with suppressed insulin signalling, will contribute to impaired glucose uptake and glycogen synthesis, and eventually, uncontrolled hepatic gluconeogenesis, ultimately resulting in systemic insulin resistance, a feature of MASLD[56]. Our results further confirmed the enhanced expression of *Ptpn1* (commonly referred to as PTP1B), known to suppress insulin signalling via dephosphorylation of both the insulin receptor and IRS-1[57]. Studies in PTP1B knock-out mice demonstrated that loss of PTP1B expression protects against HFD-induced increase in the expression of lipogenic genes in the liver[58], while a PTP1B inhibitor correspondingly reduced hepatic lipid accumulation in HFD-fed mice[59]. Based on the current and previous evidence, it can be proposed that AdipoR2 and PTP1B could be investigated as potential therapeutic targets for HFD-induced MASLD. Cytokines and chemokines play a crucial role in the inflammatory process, contributing to the development of MASLD. While chemokines are involved in the recruitment of immune cells to the site of infection, cytokines mediate and regulate the immune response, contributing to hepatocyte injury and fibrosis. Our study identified a cluster of vital proinflammatory genes activated in response to HFD feeding, leading to increased expression of numerous chemokines and cytokines (Table 2). This heightened proinflammatory response is known to aggravate liver injury[23–32]. Our study presented a comprehensive chemokine expression profile, highlighting the upregulation of multiple C-C motif and C-X-C motif chemokines (e.g., *Ccl7*, *Ccl19*, *Ccl21*, *Ccl22*, *Cxcl3*, *Cxcl9)* that are not commonly discussed in the context of MASLD progression. While *Ccl2 (MCP-1)* is well recognized in MASLD, the marked increase in *Ccl7* (11.09-fold), *Cxcl3* (12.89-fold), and *Cxcl9* (14.11-fold) suggests a more intricate macrophage and neutrophil recruitment process, which could be a novel inflammatory pathway contributing to liver damage. It is also noteworthy that the significant upregulation of *Ifnγ* (25.84-fold) may suggest a dominant role of Th1-mediated immune responses, which has been underexplored in MASLD. STRING analysis confirmed a strong interaction between *Ifnγ*, *TNfα*, *Ppary* and *Irs1*, suggesting that these genes likely influence one another and thus act in a common pathway linked to MASLD progression. PTP1B also plays complex roles in the immune system and inflammatory processes[60], and the HFD-induced increase in Ptpn1 expression likely contributed to the overall inflammatory profile observed in the present study. Cytokines such as TNF-α, IL-1β, and Fas ligand are known to be key drivers of hepatocyte apoptosis, with caspase-3 serving as a crucial downstream mediator in this process[61]. Our findings agree with this mechanism by demonstrating increased Caspase-3 and Faslg gene expression in response to an HFD, with *Tnf-α*identified as a likely key activator. The observed upregulation of PAI-1 expression served as confirmation of MASLD/MASH progression in these animals[40]. Our data further suggests potential intervention points, such as targetting *Il6*, *Il1b*, *or Tnf-α*to reduce inflammation or restoring *AdipoR2* and *Insr* to improve insulin sensitivity.

While previous studies have explored insulin resistance and lipogenesis in MASLD, our findings provide quantitative and mechanistic insights into the inflammatory response, lipid uptake, disease progression, and cholesterol efflux. These insights could contribute to the development of a diagnostic biomarker panel. Specifically, we confirmed that *Lpl* expression is elevated in response to HFD, suggesting its potential as a marker of fatty acid accumulation in hepatocytes and its link to MASLD progression. The significant upregulation of various inflammatory markers, as well as Serpine1/PAI-1 during HFD consumption, indicates the potential of these targets as possible diagnostic markers for the transition to NASH. Furthermore, the 5.27-fold increase in *Abcg1* expression highlights a previously under-recognised mechanism in which impaired cholesterol efflux may contribute to hepatic steatosis, offering a novel perspective on MASLD pathogenesis. As such, future studies

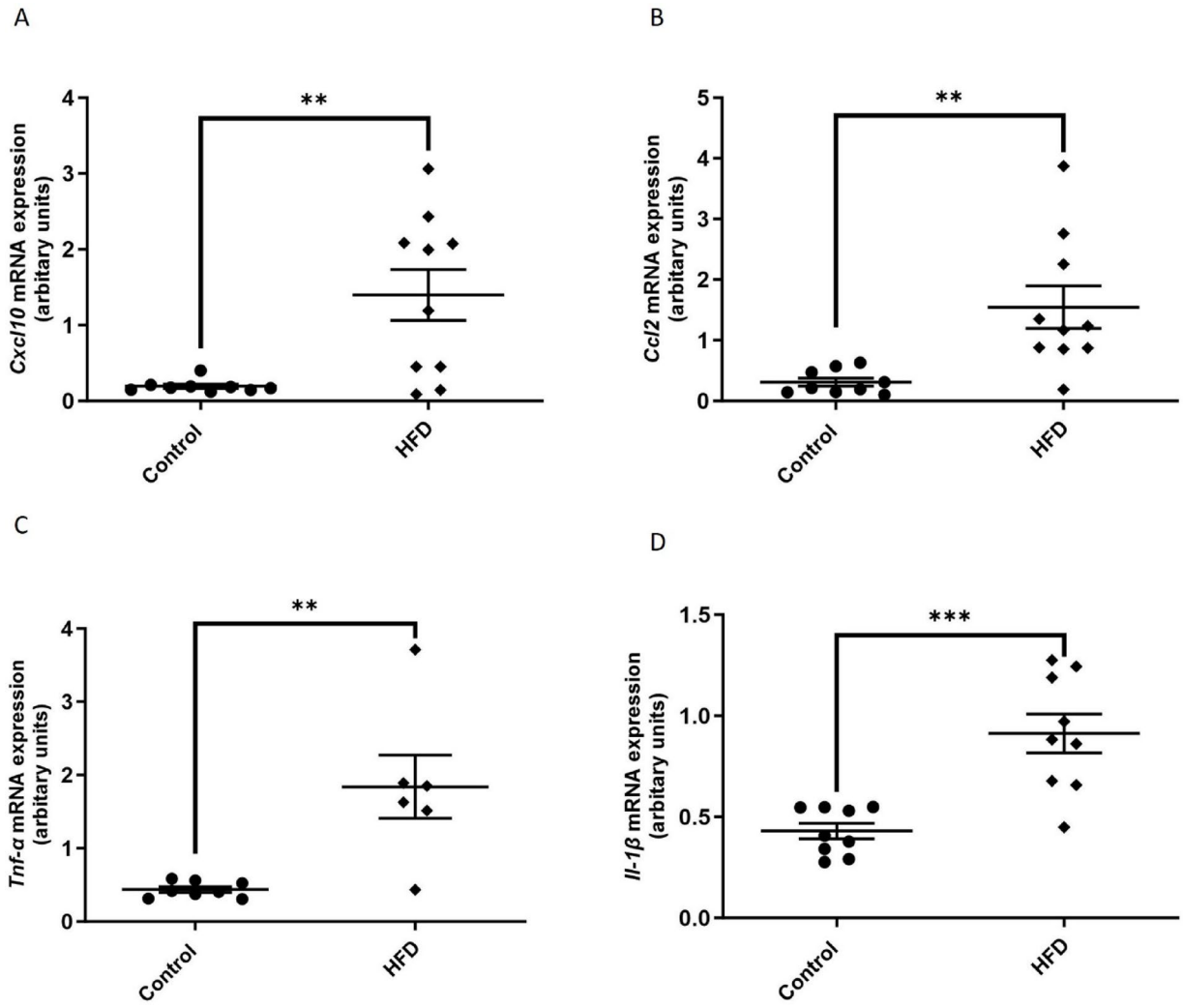

Fig. 7. Specific proinflammatory chemokines and cytokines genes are upregulated during HFD-induced MALFD. Wistar rats fed with HFD presented with increased C-X-C motif chemokine ligand 10 (*Cxcl10*) (**A**), C-C motif ligand 2 (*Ccl2*) (**B**), tumor necrosis factor-alpha (*Tnfα*) (**C**) and interleukin 1 Beta (*Il1β*) (**D**) gene expression. The findings are displayed as mean ± SEM. Significance levels are as follows: ** $p \leq 0.01$, *** $p \leq 0.001$ compared to the control rats.

will focus on investigating how modulating these pathways could translate into effective treatment strategies for MASLD and its progression to NASH.

In conclusion, the findings of this study, besides indicating that HFD dysregulates genes involved in adiponectin and insulin signalling and the DNL, identified an extensive panel of proinflammatory genes (chemokines and cytokines) and pathways (Table 2; Fig. 4), which collectively contribute to the progression of MASLD. These genes represent potential early diagnostic or therapeutic targets for mitigating MASLD. However, further research is necessary to confirm their therapeutic potential.

Data availability

All data used to support the findings of this study are included in the article. Raw data can be available on request after publication (please contact: rabia.johnson@mrc.ac.za).

Received: 17 December 2024; Accepted: 9 May 2025
Published online: 04 June 2025

References

1. Riazi, K. et al. The prevalence and incidence of NAFLD worldwide: a systematic review and meta-analysis. *Lancet Gastroenterol. Hepatol.* **7** (9), 851–861 (2022).
2. Makri, E., Goulas, A. & Polyzos, S. A. Epidemiology, pathogenesis, diagnosis and emerging treatment of nonalcoholic fatty liver disease. *Arch. Med. Res.* **52** (1), 25–37 (2021).

3. Pan, Z., Shiha, G., Esmat, G., Méndez-Sánchez, N. & Eslam, M. MAFLD predicts cardiovascular disease risk better than MASLD. *Liver Int.* (2024).
4. Lian, C-Y., Zhai, Z-Z., Li, Z-F. & Wang, L. High fat diet-triggered non-alcoholic fatty liver disease: A review of proposed mechanisms. *Chemico-Biol. Interact.* **330**, 109199 (2020).
5. Quek, J. et al. Global prevalence of non-alcoholic fatty liver disease and non-alcoholic steatohepatitis in the overweight and obese population: a systematic review and meta-analysis. *Lancet Gastroenterol. Hepatol.* **8** (1), 20–30 (2023).
6. Di Mauro, S. et al. Clinical and molecular biomarkers for diagnosis and staging of NAFLD. *Int. J. Mol. Sci.* **22** (21), 11905 (2021).
7. Reid, B. N. et al. Hepatic overexpression of hormone-sensitive lipase and adipose triglyceride lipase promotes fatty acid oxidation, stimulates direct release of free fatty acids, and ameliorates steatosis. *J. Biol. Chem.* **283** (19), 13087–13099 (2008).
8. Liu, H-J. et al. Rotundic acid ameliorates non-alcoholic steatohepatitis via SREBP-1c/SCD1 signaling pathway and modulating gut microbiota. *Int. Immunopharmacol.* **99**, 108065 (2021).
9. Park, M-Y. & Mun, S. T. Dietary carnosic acid suppresses hepatic steatosis formation via regulation of hepatic fatty acid metabolism in high-fat diet-fed mice. *Nutr. Res. Pract.* **7** (4), 294–301 (2013).
10. Wang, Z. V. & Scherer, P. E. Adiponectin, the past two decades. *J. Mol. Cell Biol.* **8** (2), 93–100 (2016).
11. Duan, Y. et al. Association of inflammatory cytokines with non-alcoholic fatty liver disease. *Front. Immunol.* **13**, 880298 (2022).
12. Day, C. P. & James, O. F. *Steatohepatitis: a Tale of Two Hits?* 842–845 (Elsevier, 1998).
13. Nakamura, A. & Terauchi, Y. Lessons from mouse models of high-fat diet-induced NAFLD. *Int. J. Mol. Sci.* **14** (11), 21240–21257 (2013).
14. Duarte, N. et al. How inflammation impinges on NAFLD: a role for Kupffer cells. *Biomed. Res. Int.* **2015** (1), 984578 (2015).
15. Peiseler, M. & Tacke, F. Inflammatory mechanisms underlying nonalcoholic steatohepatitis and the transition to hepatocellular carcinoma. *Cancers* **13** (4), 730 (2021).
16. Roehlen, N., Crouchet, E. & Baumert, T. F. Liver fibrosis: mechanistic concepts and therapeutic perspectives. *Cells* **9** (4), 875 (2020).
17. Kotzé-Hörstmann, L. et al. Characterization and comparison of the divergent metabolic consequences of high-sugar and high-fat diets in male Wistar rats. *Front. Physiol.* **13**, 904366 (2022).
18. Kotzé-Hörstmann, L., Bedada, D., Johnson, R., Mabasa, L. & Sadie-Van Gijsen, H. The effects of a green Rooibos (Aspalathus linearis) extract on metabolic parameters and adipose tissue biology in rats fed different obesogenic diets. *Food Funct.* **13** (24), 12648–12663 (2022).
19. Folch, J., Lees, M. & Stanley, G. S. A simple method for the isolation and purification of total lipides from animal tissues. *J. Biol. Chem.* **226** (1), 497–509 (1957).
20. Boehm, O. et al. Clinical chemistry reference database for Wistar rats and C57/BL6 mice. (2007).
21. Kirsch, R. et al. Rodent nutritional model of non-alcoholic steatohepatitis: species, strain and sex difference studies. *J. Gastroenterol. Hepatol.* **18** (11), 1272–1282 (2003).
22. Shabalala, S. C. et al. The effect of adiponectin in the pathogenesis of non-alcoholic fatty liver disease (NAFLD) and the potential role of polyphenols in the modulation of adiponectin signaling. *Biomed. Pharmacother.* **131**, 110785 (2020).
23. Nagata, N., Chen, G., Xu, L. & Ando, H. An update on the chemokine system in the development of NAFLD. *Medicina* **58** (6), 761 (2022).
24. Marra, F. & Tacke, F. Roles for chemokines in liver disease. *Gastroenterology* **147** (3), 577–594 (2014). e1.
25. Nam, H. H. et al. Granulocyte colony stimulating factor treatment in non-alcoholic fatty liver disease: beyond marrow cell mobilization. *Oncotarget* **8** (58), 97965 (2017).
26. Chen, W., Zhang, J., Fan, H-N. & Zhu, J-S. Function and therapeutic advances of chemokine and its receptor in nonalcoholic fatty liver disease. *Therapeutic Adv. Gastroenterol.* **11**, 1756284818815184 (2018).
27. Li, J. et al. IFN-γ contributes to the hepatic inflammation in HFD-induced nonalcoholic steatohepatitis by STAT1β/TLR2 signaling pathway. *Mol. Immunol.* **134**, 118–128 (2021).
28. Hadinia, A., Doustimotlagh, A. H., Goodarzi, H. R., Arya, A. & Jafarinia, M. Circulating levels of pro-inflammatory cytokines in patients with nonalcoholic fatty liver disease and non-alcoholic steatohepatitis. *Iran. J. Immunol.* **16** (4), 327–333 (2019).
29. Kountouras, J. et al. Innate immunity and nonalcoholic fatty liver disease. *Annals Gastroenterol.* **36** (3), 244 (2023).
30. Liu, J. et al. Decoding the role of immune T cells: A new territory for improvement of metabolic-associated fatty liver disease. *Imeta* **2** (1), e76 (2023).
31. Friedline, R. H. et al. IFNγ-IL12 axis regulates intercellular crosstalk in metabolic dysfunction-associated steatotic liver disease. *Nat. Commun.* **15** (1), 5506 (2024).
32. Coste, S-C. et al. Metabolic Dysfunction-Associated steatotic liver disease: the associations between inflammatory markers, TLR4, and cytokines IL-17A/F, and their connections to the degree of steatosis and the risk of fibrosis. *Biomedicines* **12** (9), 2144 (2024).
33. Yu, T. et al. Gut Microbiota–NLRP3 inflammasome crosstalk in metabolic dysfunction-associated steatotic liver disease. *Clin. Res. Hepatol. Gastroenterol.* 102458. (2024).
34. Ullah, A., Singla, R. K., Batool, Z., Cao, D. & Shen, B. Pro-and anti-inflammatory cytokines are the game-changers in childhood obesity-associated metabolic disorders (diabetes and non-alcoholic fatty liver diseases). *Rev. Endocr. Metab. Disord.* 1–21. (2024).
35. Cho, W. et al. Interleukin-27 as a novel player in alleviating hepatic steatosis: mechanistic insights from an in vitro analysis. *Biochem. Biophys. Res. Commun.* **703**, 149671 (2024).
36. Alkhouri, N. et al. Circulating soluble Fas and Fas ligand levels are elevated in children with nonalcoholic steatohepatitis. *Dig. Dis. Sci.* **60**, 2353–2359 (2015).
37. Thapaliya, S. et al. Caspase 3 inactivation protects against hepatic cell death and ameliorates fibrogenesis in a diet-induced NASH model. *Dig. Dis. Sci.* **59**, 1197–1206 (2014).
38. Westerbacka, J. et al. Genes involved in fatty acid partitioning and binding, lipolysis, monocyte/macrophage recruitment, and inflammation are overexpressed in the human fatty liver of insulin-resistant subjects. *Diabetes* **56** (11), 2759–2765 (2007).
39. Heeren, J. & Scheja, L. Metabolic-associated fatty liver disease and lipoprotein metabolism. *Mol. Metabolism*. **50**, 101238 (2021).
40. Zhao, Y. et al. Transcriptomics reveal a molecular signature in the progression of nonalcoholic steatohepatitis and identifies PAI–1 and MMP–9 as biomarkers in in vivo and in vitro studies. *Mol. Med. Rep.* **29** (1), 15 (2023).
41. Chen, Z., Yu, R., Xiong, Y., Du, F. & Zhu, S. A vicious circle between insulin resistance and inflammation in nonalcoholic fatty liver disease. *Lipids Health Dis.* **16**, 1–9 (2017).
42. Vitulo, M. et al. Current therapeutical approaches targeting lipid metabolism in NAFLD. *Int. J. Mol. Sci.* **24** (16), 12748 (2023).
43. Tsay, A. & Wang, J-C. The role of PIK3R1 in metabolic function and insulin sensitivity. *Int. J. Mol. Sci.* **24** (16), 12665 (2023).
44. Chadt, A. & Al-Hasani, H. Glucose transporters in adipose tissue, liver, and skeletal muscle in metabolic health and disease. *Pflügers Archiv-European J. Physiol.* **472** (9), 1273–1298 (2020).
45. Koren, S. & Fantus, I. G. Inhibition of the protein tyrosine phosphatase PTP1B: potential therapy for obesity, insulin resistance and type-2 diabetes mellitus. *Best Pract. Res. Clin. Endocrinol. Metab.* **21** (4), 621–640 (2007).
46. Nogueira-Ferreira, R., Oliveira, P. F. & Ferreira, R. *Liver Metabolism: the Pathways Underlying Glucose Utilization and Production* 141–156 (Elsevier, 2024).
47. Vesković, M. et al. The interconnection between hepatic insulin resistance and metabolic dysfunction-associated steatotic liver disease—the transition from an adipocentric to liver-centric approach. *Curr. Issues. Mol. Biol.* **45** (11), 9084–9102 (2023).
48. Son, Y. et al. Ameliorative effect of Annona muricata (Graviola) extract on hyperglycemia induced hepatic damage in type 2 diabetic mice. *Antioxidants* **10** (10), 1546 (2021).

49. Neshat, S. Y., Quiroz, V. M., Wang, Y., Tamayo, S. & Doloff, J. C. Liver disease: induction, progression, immunological mechanisms, and therapeutic interventions. *Int. J. Mol. Sci.* **22** (13), 6777 (2021).
50. Manikat, R., Ahmed, A. & Kim, D. Up-to-date global epidemiology of nonalcoholic fatty liver disease. *Hepatobiliary Surg. Nutr.* **12** (6), 956 (2023).
51. Vancells Lujan, P., Vinas Esmel, E. & Sacanella Meseguer, E. Overview of non-alcoholic fatty liver disease (NAFLD) and the role of sugary food consumption and other dietary components in its development. *Nutrients* **13** (5), 1442 (2021).
52. Xu, Z-J., Fan, J-G., Ding, X-D., Qiao, L. & Wang, G-L. Characterization of high-fat, diet-induced, non-alcoholic steatohepatitis with fibrosis in rats. *Dig. Dis. Sci.* **55**, 931–940 (2010).
53. Khatoon, S. et al. Apigenin-6-C-glucoside ameliorates MASLD in rodent models via selective agonism of adiponectin receptor 2. *Eur. J. Pharmacol.* **978**, 176800 (2024).
54. Esler, W. P. & Cohen, D. E. Pharmacologic Inhibition of lipogenesis for the treatment of NAFLD. *J. Hepatol.* **80** (2), 362–377 (2024).
55. Gamberi, T., Magherini, F., Modesti, A. & Fiaschi, T. Adiponectin signaling pathways in liver diseases. *Biomedicines* **6** (2), 52 (2018).
56. Samuel, V. T. & Shulman, G. I. The pathogenesis of insulin resistance: integrating signaling pathways and substrate flux. *J. Clin. Investig.* **126** (1), 12–22 (2016).
57. Ravichandran, L. V., Chen, H., Li, Y. & Quon, M. J. Phosphorylation of PTP1B at Ser50 by Akt impairs its ability to dephosphorylate the insulin receptor. *Mol. Endocrinol.* **15** (10), 1768–1780 (2001).
58. Delibegovic, M. et al. Liver-specific deletion of protein-tyrosine phosphatase 1B (PTP1B) improves metabolic syndrome and attenuates diet-induced Endoplasmic reticulum stress. *Diabetes* **58** (3), 590–599 (2009).
59. Li, J. et al. CX08005, a protein tyrosine phosphatase 1b inhibitor, attenuated hepatic lipid accumulation and microcirculation dysfunction associated with nonalcoholic fatty liver disease. *Pharmaceuticals* **16** (1), 106 (2023).
60. Read, N. E. & Wilson, H. M. Recent developments in the role of protein tyrosine phosphatase 1B (PTP1B) as a regulator of immune cell signalling in health and disease. *Int. J. Mol. Sci.* **25** (13), 7207 (2024).
61. Eguchi, A., Wree, A. & Feldstein, A. E. Biomarkers of liver cell death. *J. Hepatol.* **60** (5), 1063–1074 (2014).

Acknowledgements

Grant holders acknowledge that the authors' opinions, findings, conclusions, or recommendations expressed in any publication generated by the SAMRC-supported research. The SAMRC accepts no liability for any inaccuracy whatsoever. We want to acknowledge the technical staff at the SAMRC Biomedical and Research Innovation Platform (BRIP).

Author contributions

RJ and HVG: Conceptualization, Funding acquisition, Formal analysis, and Writing - Original Draft. SS: Investigation. LK-H and HVG: Resources (Experimental animals). RJ, HVG, SS, JS, CP, AA, L K-H, L M, N S and PR: Writing - Review & Editing. Afolake Arowolo: Visualization (Image preparation), Writing and Editing.

Funding

This research was supported by funding from the National Research Foundation (NRF) Competitive Program for rated Researchers to RJ (CPRR Grant numbers: SRUG2203301281), NRF Support for Y-rated researchers (Grant number 112244), the South African Rooibos Council, and baseline funding from the Biomedical Research and Innovation Platform of the South African Medical Research Council (SAMRC). The NRF Professional Development Program funded Dr Shabalala. The authors are solely responsible for the content, which does not necessarily reflect the official views of the funders.

Declarations

Competing interests

The authors declare no competing interests.

Ethics approval and consent to participate

All experimental methods were performed in accordance with the Guide for the Care and Use of Laboratory Animals of the National Institute of Health (NIH, 8th Edition, 2011), the Animal Research: Reporting of In vivo Experiments (ARRIVE) guidelines, which were approved by the Animal Research Ethics Committees at Stellenbosch University (SU-ACU-2018-6786) and the University of Zululand (PGD2017/206).

Consent for publication

All authors have read, reviewed and agreed to the published version of the manuscript.

Additional information

Supplementary Information The online version contains supplementary material available at https://doi.org/10.1038/s41598-025-02001-2.

Correspondence and requests for materials should be addressed to R.J.